

# **Neuronal and glial glycine transporters have different stoichiometries**

Michel J. Roux and Stéphane Supplisson<sup>†</sup>

Laboratoire de Neurobiologie  
Unité Mixte de Recherche 8544  
Centre National de la Recherche Scientifique  
École Normale Supérieure  
46 rue d'Ulm  
75230 Paris cedex 05  
France

<sup>†</sup> Corresponding author

Tel: ++ 33 1 44 32 38 94

Fax: ++ 33 1 44 32 38 87

email: [supplis@wotan.ens.fr](mailto:supplis@wotan.ens.fr)

## Summary

**A neurotransmitter transporter can potentially mediate uptake or release of substrate, and its stoichiometry is a key factor that controls the driving force and thus the neurotransmitter flux direction. We have used a combination of electrophysiology and radio-tracing techniques to evaluate the stoichiometries of two glycine transporters involved in glycinergic or glutamatergic transmission. We show that GlyT2a, a transporter present in glycinergic boutons, has a stoichiometry of 3 Na<sup>+</sup>/Cl<sup>-</sup>/glycine which predicts effective glycine accumulation in all physiological conditions. GlyT1b, a glial transporter, has a stoichiometry of 2 Na<sup>+</sup>/Cl<sup>-</sup>/glycine which predicts that glycine can be exported or imported depending on physiological conditions. GlyT1b may thus modulate glutamatergic synapses by increasing or decreasing the glycine concentration around NMDA receptors.**

**Running title:** Glycine transporters stoichiometries

## Introduction

The glycine transporters identified in the CNS are likely to play roles both at inhibitory glycinergic synapses, where glycine activates low affinity strychnine-sensitive chloride-permeable receptors (GlyRs) (Aprison and Werman, 1965; Grenningloh et al., 1987) and at glutamatergic synapses (Ascher, 1990; Attwell et al., 1993), where glycine plays a facilitatory role as a high affinity co-agonist with glutamate of *N-methyl-D*-aspartate receptors (NMDAR) (Johnson and Ascher, 1987; see review in Danysz and Parsons, 1998). In brain stem and spinal cord, glycine uptake does not influence the time-course of inhibitory post-synaptic currents (Titmus et al., 1996;

## Glycine transporters stoichiometries

Singer and Berger, 1999) and the function of glycine transporters is to ensure a rapid re-supply of pre-synaptic terminals (Zafra et al., 1997) and perhaps to limit inter-synaptic spill-over (see review in Bergles et al., 1999). In excitatory transmission, the capacity of glycine transporters to keep the local extracellular glycine concentration ( $[Gly]_o$ ) below saturating levels for NMDARs has been demonstrated in a few cases, such as in a model system where glycine transporters and NMDARs were co-expressed in *Xenopus* oocytes (Supplisson and Bergman, 1997) and in slices of brain stem (Berger et al., 1998) and hippocampus (Bergeron et al., 1998). In principle, this should allow potentiation of NMDARs by sudden increases of extracellular glycine. Such rises may come from glycine spill-over from nearby glycinergic terminals (Fern et al., 1996). Another possible origin is reverse uptake where transporters become a calcium-independent source of glycine. Because of the reduction of  $Na^+$  and  $Cl^-$  electrochemical gradients during ischemic conditions, reverse transport may also be the cause of the massive liberation of glycine which has been observed (Baker et al., 1991).

Many glycine transporters have been cloned in the CNS of mammals. All are members of the  $Na^+/Cl^-$ -coupled symport family and derive from two genes, GlyT1 and GlyT2. The three GlyT1 isoforms (GlyT1a-c) differ only in their short N-termini. The GlyT2 isoforms (GlyT2a-b) have an additional ~200 amino-acid long N-terminus and have a 48% identity with GlyT1 in their overlapping sequence (reviewed in Palacin et al., 1998).

The cellular and tissue localization of the various GlyT subtypes appears to be finely regulated (Borowsky and Hoffman, 1998). In spinal cord, brain stem and cerebellum, GlyT2 has been found to be a reliable marker of glycinergic neurons both by *in situ* hybridization (Adams et al., 1995; Luque et al., 1995; Zafra et al., 1995) and

## Glycine transporters stoichiometries

immunocytochemistry studies (Jursky and Nelson, 1995; Zafra et al., 1995; Spike et al., 1997). GlyT2 is detected in all glycinergic boutons but outside the active zones (Spike et al., 1997). In contrast, GlyT1 is located in fine astroglial processes both around glycinergic terminals (Zafra et al., 1995) and in areas devoid of strychnine-sensitive receptors (Smith et al., 1992; Zafra et al., 1995).

In the present paper, we investigate the stoichiometry and kinetic properties of GlyT1b and GlyT2a to understand how these two transporters achieve their specific functions in neurons and glia. Immunocytochemistry studies have shown that glycinergic neurons, both in situ (Storm-Mathisen and Ottersen, 1990) and in culture (Poyatos et al., 1997), have a higher glycine content than glial cells. This difference is also observed in transfected cells expressing either GlyT1 or GlyT2 (Poyatos et al., 1997). A high level of glycine in glycinergic terminals actually appears to be a requirement for effective filling of the synaptic vesicles, because of the low affinity of the vesicular inhibitory amino-acid transporter VIAAT (Sagne et al., 1997).

To date, conclusive stoichiometries have been established under voltage-clamp conditions only for a few transporters such as the glutamate transporters EAAT3 (Zerangue and Kavanaugh, 1996) and GLT-1 (Levy et al., 1998), and the epithelial  $\text{Na}^+$ /glucose transporter SGLT1 (Mackenzie et al., 1998). Based on earlier work on reconstituted vesicles with GABA transporters (Radian and Kanner, 1983), it is generally assumed that most of  $\text{Na}^+$ / $\text{Cl}^-$ -coupled transporters have a stoichiometry of 2  $\text{Na}^+$ / $\text{Cl}^-$  per substrate molecule (see reviews in Kanner and Schuldiner, 1987; Palacin et al., 1998). In the present study, we show that this prediction is correct for GlyT1b, but that the neuronal GlyT2a transports an additional  $\text{Na}^+$  ion. We also show that GlyT2a reverse transport is limited compared to that of GlyT1b. These two differences indicate that GlyT1b has the properties expected for a transporter

controlling the extracellular glycine concentration and thus tonically modulating NMDARs, whereas GlyT2a appears adapted to accumulate glycine into pre-synaptic terminals.

### Results

#### GlyT1b and GlyT2a Have a Different Charge / Glycine Ratio

In voltage-clamped *Xenopus* oocytes expressing either GlyT1b (Figure 1A) or GlyT2a (Figure 1B), glycine (25  $\mu$ M) evokes a maintained inward current ( $I_T$ ) which requires both  $\text{Na}^+$  and  $\text{Cl}^-$  ions. To measure the net number of charges translocated with each glycine molecule ( $z_T$ ), we compared the time integral of the glycine-induced current ( $Q_T$ ) with the simultaneous  $^{14}\text{C}$  glycine uptake ( $J_{\text{Gly}}$ ). Like the current induced by glycine, the radioactive flux required both  $\text{Na}^+$  and  $\text{Cl}^-$ .

When  $^{14}\text{C}$  glycine uptake was measured in the presence of  $\text{Na}^+$  and  $\text{Cl}^-$  and plotted as a function of  $Q_T$ , a striking difference was observed between the two transporters. Figure 1C shows the linear relationship between  $Q_T$  (shaded in Figure 1A-B) and the corresponding glycine uptake for various expression levels in GlyT1b<sup>+</sup> or GlyT2a<sup>+</sup> oocytes, for holding potentials ranging from -120 to 0 mV. The slope

$z_T = \frac{Q_T}{F J_{\text{Gly}}}$ , where  $F$  is the Faraday constant, is  $1.01 \pm 0.04$  elementary charge ( $e_0$ ) / glycine ( $n = 20$ ) for GlyT1b and  $2.14 \pm 0.17 e_0$  / glycine ( $n = 20$ ) for GlyT2a. The charge / glycine ratio was voltage-independent between -120 and 0 mV for GlyT1b but for GlyT2a,  $z_T$  increased slightly with hyperpolarization from  $1.9 e_0$  at 0 mV to  $2.3 e_0$  at -120 mV.

A net charge of +1 per glycine for GlyT1b is in perfect agreement with the stoichiometry of 2  $\text{Na}^+/\text{Cl}^-$ /glycine determined for native transporters in reconstituted

## Glycine transporters stoichiometries

membrane vesicles (Zafra and Gimenez, 1986; Aragon et al., 1987). In contrast, a net charge per glycine of +2 for GlyT2a could be explained by one of the following mechanisms: an uncoupled conductance activated by glycine, the co-transport of 3 Na<sup>+</sup> ions or a zero net flux for Cl<sup>-</sup> (assuming that no ions other than Na<sup>+</sup> and Cl<sup>-</sup> are involved). To rule out the last hypothesis, we simultaneously measured Cl<sup>-</sup> uptake and  $Q_T$ . To minimize the Cl<sup>-</sup> fluxes not linked to glycine uptake, oocytes were held at -30 mV, close to  $E_{Cl}$ .  $Q_T$  was proportional to <sup>36</sup>Cl<sup>-</sup> uptake with ratios of  $0.93 \pm 0.06 e_0/Cl^-$  (n = 8) and  $2.07 \pm 0.04 e_0/Cl^-$  (n = 17) for GlyT1b and GlyT2a, respectively. Using the previously determined values of  $z_T$ , these results lead to identical ratios of 1.05 and 1.03 Cl<sup>-</sup> per glycine for the two transporters (Figure 1D). To investigate further the origin of this difference in charge / glycine ratios, we analyzed some of the kinetic properties of both transporters.

### **Uptake Current as a Function of Membrane Potential**

In control solution, voltage jumps revealed slow transient currents in both GlyT1b<sup>+</sup> (Figure 2A) and GlyT2a<sup>+</sup> oocytes (Figure 2E) that were absent in non-injected oocytes. These transients disappeared when saturating glycine concentrations were applied (Figures 2B and 2F). Thus, as for other Na<sup>+</sup>-coupled transporters, transient currents are negatively-coupled to steady-state uptake currents (Loo et al., 1993; Mager et al., 1993). They will be analyzed in detail in a subsequent paper.

Applications of glycine at high concentrations (200 μM - 1 mM) induced inward currents at all potentials tested (Figures 2B and 2F). The transport currents  $I_T$  were isolated by subtraction of the steady-state currents recorded in the absence of glycine (diamonds) from those recorded in its presence (circles). The  $I_T$ -voltage

## Glycine transporters stoichiometries

relationships were quasi-ohmic for both transporters (Figures 2D and 2H), but GlyT1b  $I_T$  displayed a small inward rectification at positive potentials. No current inversion was observed for either transporter.

### **GlyT1b and GlyT2a Have Similar Apparent Glycine Affinities**

The uptake currents of GlyT1b and GlyT2a evoked by rapid superfusion of glycine at various concentrations were recorded at different potentials using the voltage-step protocol described in figure 2A-B (Figure 3A-B). To limit the depletion of juxtamembrane glycine at low concentrations (see Supplisson and Bergman, 1997), only oocytes with low expression levels ( $|I_{T\max}| < 200$  nA and 400 nA at  $V_m = -40$  mV for GlyT1b and GlyT2a, respectively) were considered. In these conditions, the dose response curves could be fitted using a Michaelis-Menten equation at all potentials.

The glycine concentrations producing half-maximal responses ( $K_{0.5}^{Gly}$ ) were voltage-independent at potentials more negative than  $-50$  mV (Figure 3C) and had similar values for the two transporters ( $22.6 \pm 2.5$   $\mu$ M ( $n = 6$ ) and  $24.6 \pm 2.3$   $\mu$ M ( $n = 12$ ) for GlyT1b and GlyT2a, respectively). At potentials more positive than  $-50$  mV,  $K_{0.5}^{Gly}$  increased with the membrane potential. The voltage dependence was steeper for GlyT2a than for GlyT1b, with equivalent charges when fitted with Boltzmann distributions of  $0.78 \pm 0.03$   $e_0$  ( $n = 6$ ) and  $1.38 \pm 0.07$   $e_0$ , ( $n = 12$ ) for GlyT1b and GlyT2a, respectively.

### **GlyT2a Has a Higher Hill Coefficient for Na<sup>+</sup> than GlyT1b**

Uptake currents of GlyT1b and GlyT2a were recorded as a function of  $[Na^+]_o$  and membrane potential using a saturating (1 mM) glycine concentration (Figure 3D-E). In these experiments, choline was substituted for Na<sup>+</sup> to maintain a constant

## Glycine transporters stoichiometries

monovalent cation concentration. When Na<sup>+</sup> was completely replaced by choline, no transporter-mediated glycine uptake was observed and the transporter-specific transient currents observed in absence of glycine but presence of Na<sup>+</sup> (Figures 2A and 2E) also disappeared, suggesting that choline does not interact with the transporters.

At -130 mV, the  $K_{0.5}^{Na}$  of GlyT1b was  $5.9 \pm 0.5$  mM ( $n = 5$ ), about half that of GlyT2a ( $10.2 \pm 0.2$  mM,  $n = 4$ ) (Figure 3F). The  $K_{0.5}^{Na}$  of GlyT2a increased steeply with voltage. When fitted with a Boltzmann distribution, the voltage-dependence of the  $K_{0.5}^{Na}$  were described by equivalent charges of  $0.25 \pm 0.04 e_0$  ( $n = 5$ ) and  $0.56 \pm 0.04 e_0$  ( $n = 4$ ) for GlyT1b and GlyT2a, respectively.

The Na<sup>+</sup> Hill coefficient of GlyT1b had a mean value of  $1.41 \pm 0.02$  ( $n = 5$ ). In contrast, the Hill coefficient of GlyT2a was consistently close to or higher than 2 ( $2.21 \pm 0.05$ ,  $n = 4$ , from -130 to 0 mV,  $p < .001$ ) (Figure 3G).

### **The Difference in Stoichiometry is Confirmed by the Determination of the Reversal Potential as a Function of [Na<sup>+</sup>]<sub>o</sub> and [Gly]<sub>o</sub>**

The fact that the Hill coefficients estimated from the Na<sup>+</sup> activation curves were  $< 2$  for GlyT1b but  $> 2$  for GlyT2a, together with the difference in charge / glycine ratios, suggested that GlyT2a co-transporters a higher number of Na<sup>+</sup> ions. To address directly this question, we set out to measure the equilibrium potentials of GlyT1b and GlyT2a and the changes produced by alterations of [Na<sup>+</sup>]<sub>o</sub>, [Cl<sup>-</sup>]<sub>o</sub> and [Gly]<sub>o</sub>.

The equilibrium potential of a glycine transporter depends on the ionic and substrate electrochemical gradients as indicated by the thermodynamic relation:

$$E_T = \frac{2.3 R T}{(n_{Na} - n_{Cl}) F} \log \left( \frac{[Na^+]_o^{n_{Na}} [Cl^-]_o^{n_{Cl}} [Gly]_o}{[Na^+]_i^{n_{Na}} [Cl^-]_i^{n_{Cl}} [Gly]_i} \right) \quad (1)$$

## Glycine transporters stoichiometries

where  $R$ ,  $T$  and  $F$  have their usual meanings and  $n_{\text{Na}}$  and  $n_{\text{Cl}}$  indicate, respectively, the number of  $\text{Na}^+$  and  $\text{Cl}^-$  ions coupled to the transport of each glycine molecule.

Decreasing the driving force is necessary to allow measurement of  $E_T$  in a practical voltage range. Because outward current could not be detected with GlyT2a in experiments using low  $[\text{Na}^+]_o$  or low  $[\text{Cl}^-]_o$ , we chose to manipulate the intracellular concentrations. In the following experiments, voltage-clamped GlyT1b<sup>+</sup> or GlyT2a<sup>+</sup> oocytes were impaled with a nanoliter injector micropipette and controlled volumes (4-16 nl) of solutions containing either glycine (1 M) alone or glycine (1 M) and NaCl (1 M) were injected prior to recording  $I_T$  as a function of either  $[\text{Na}^+]_o$ ,  $[\text{Cl}^-]_o$  or  $[\text{Gly}]_o$  (Figure 4C). For subtraction of the oocytes background current, we used two specific glycine uptake inhibitors of GlyT1b and GlyT2a (ORG24598 and ORG26176, respectively (Walker et al., 1999)) which blocked all, inward and outward, glycine-evoked current (Figure 4A-B). The mean glycine-evoked current inhibitions ( $[\text{Gly}]_o = 200 \mu\text{M}$ ,  $V_H = -40 \text{ mV}$ ) with 5  $\mu\text{M}$  ORG24598 and ORG26176 were  $100.1 \pm 0.5\%$  ( $n = 4$ ) and  $101.6 \pm 1.8\%$  ( $n = 4$ ), respectively. These percentages of inhibition confirm the absence of uncoupled currents over the range of measured  $E_{\text{Rev}}$ , as found also in substitution experiments where  $\text{Na}^+$  or  $\text{Cl}^-$  were replaced by choline or gluconate. In this condition, it is reasonable to assume that the current reversal potential ( $E_{\text{Rev}}$ ) corresponds to the transport equilibrium potential,  $E_T$ .

Microinjections of glycine (4-16 nl) were sufficient to evoke large outward currents in GlyT1b<sup>+</sup> oocytes at  $V_H = -40 \text{ mV}$  (Figure 4A, middle trace). In contrast, outward currents were never detected after injection of glycine alone in GlyT2a<sup>+</sup> oocytes (Figure 4A, bottom trace), though the injection produced a marked decrease of the inward uptake current indicating the reduction of the driving force for influx. It was only when glycine and NaCl were co-injected that outward currents were evoked

## Glycine transporters stoichiometries

in GlyT2a<sup>+</sup> oocytes (Figure 4B, bottom trace). Following such combined injection, a transient inward current was always observed in either non-injected oocytes, GlyT1b<sup>+</sup> or GlyT2a<sup>+</sup> oocytes indicating that this transient current is unrelated to glycine transporters expression (Figure 4B). Once the transient current had subsided, steady outward currents were observed at  $V_H = -40$  mV for both transporters, suggesting that the intracellular concentrations of glycine, Na<sup>+</sup> and Cl<sup>-</sup> did not change significantly during the time of the experiment (9 to 15 minutes post-injection). Oocytes in which the injection produced a non specific increase in currents at all potentials were not considered.

A direct evaluation of stoichiometry was obtained by studying  $E_{Rev}$  changes as a function of the external concentration of a given transported ligand  $[X]_o$ . With all other factors being constant, equation 1 can be simplified to  $E_T = a_X \log([X]_o) + b_X$ , where the slope  $a_X = 2.3 R T n_X / (z_T F)$  depends on  $z_T$  and  $n_X$ , the stoichiometry of the coupled variable (Zerangue and Kavanaugh, 1996). Thus, for a tenfold change in external glycine concentration, the predicted changes in  $E_T$  at 23°C are 58 and 29 mV for  $z_T = 1$  and  $z_T = 2$ , respectively. These values agree with the changes in  $E_{Rev}$  between 10 and 100  $\mu$ M glycine that were of  $61.0 \pm 4.2$  mV ( $n = 7$ ) and  $28.2 \pm 1.8$  mV ( $n = 12$ ) for GlyT1b (injection of 16 nmol of glycine) and GlyT2a (injection of 16 nmol of NaCl + glycine), respectively. The GlyT1b/GlyT2a slope ratio is 2.16 close to the value of 2.12 calculated from the experimental charge / glycine ratio. This result confirms that the additional charge of GlyT2a is thermodynamically coupled to transport. As expected, the  $E_{Rev}$  slopes determined when  $[Cl^-]_o$  was changed from 100 to 33 and 10mM were  $58.6 \pm 6.1$  mV ( $n = 7$ ) and  $36.3 \pm 0.9$  mV ( $n = 8$ ) for GlyT1b and GlyT2a, respectively. This gives  $n_{Cl} = 1.0$  for GlyT1b and  $n_{Cl} = 1.2$  for GlyT2a, confirming that 1 Cl<sup>-</sup> is transported per glycine molecule as determined

## Glycine transporters stoichiometries

previously with flux experiments (Figure 1D).

To determine the  $\text{Na}^+$  coupling, we recorded the  $I_T$ - $V_m$  relationships for four  $\text{Na}^+$  concentrations in the presence of 100  $\mu\text{M}$  glycine. Results of representative experiments with GlyT1b<sup>+</sup> and GlyT2a<sup>+</sup> oocytes are shown Figure 5A and 5B respectively. For GlyT1b, the slope of  $E_T = f(\log[\text{Na}^+]_o)$  was  $a_{\text{Na}} = 114.7 \pm 8.1$  mV ( $n = 10$ ) per tenfold  $\text{Na}^+$  concentration change, which, considering that  $z_T = 1$ , gave a number of  $\text{Na}^+$  ions per glycine of  $n_{\text{Na}} = 2.0 \pm 0.1$  (Figure 5C). For GlyT2a, the slope was  $a_{\text{Na}} = 91.6 \pm 4.6$  mV ( $n = 8$ ), giving  $n_{\text{Na}} = 3.1 \pm 0.1$ , considering  $z_T = 2$  (Figure 5D). The slopes are close to the theoretical predictions of 118 mV and 87 mV for  $2\text{Na}^+ / 1\text{Cl}^- / 1\text{gly}$  and  $3\text{Na}^+ / 1\text{Cl}^- / 1\text{gly}$ , respectively. The difference in  $n_{\text{Na}}$  confirms that the additional charge of GlyT2a is carried by a third  $\text{Na}^+$  ion coupled to glycine uptake.

### **Neuronal and Glial Glycine Transporters Have Different Reverse Transport Kinetics**

The inward rectification of GlyT2a  $I_T$ - $V_m$  (Figure 5B) compared to the linear GlyT1b  $I_T$ - $V_m$  (Figure 5A) observed at low external  $\text{Na}^+$  suggested that the two transporters may have different reverse transport characteristics. This was confirmed in experiments where transient intracellular accumulations of glycine were induced by superfusion of the oocytes under voltage-clamp with a saturating glycine concentration for 1 to 3 minutes (Figure 6A-C). The steady-state currents of GlyT1b<sup>+</sup> and GlyT2a<sup>+</sup> oocytes recorded in absence of glycine prior ( $I_1$ ) and after ( $I_2$ ) glycine application (1mM) were plotted as a function of time (Figure 6A). With GlyT1b<sup>+</sup> oocytes, glycine accumulation ( $0.29 \pm .05$  nmol,  $n = 15$ ) evoked a net outward current ( $I_2 - I_1$ ) upon glycine removal which increased exponentially with depolarization, as shown in the

## Glycine transporters stoichiometries

current-voltage relationship of figure 6B. These outward currents were blocked by ORG24958 (not shown) and their amplitudes increased with glycine uptake (Figure 6C). The presence of a large scatter in figure 6C suggested that variation in the basal intracellular  $\text{Na}^+$ ,  $\text{Cl}^-$  or glycine concentrations of individual oocytes may alter the efflux rate. In contrast, similar glycine accumulations in GlyT2a<sup>+</sup> oocytes ( $0.25 \pm .03$  nmol,  $n = 11$ ) did not evoke an outward current at any of the potentials tested (Figure 6A left panel and 6B), even when  $\text{Na}^+$  was replaced by  $\text{Li}^+$  (data not shown).

These experiments demonstrate that following a comparable glycine load (Figure 6C), glycine is exported at a significant rate from GlyT1b<sup>+</sup> oocytes but not from GlyT2a<sup>+</sup>. This suggests either that the GlyT2a apparent affinities for intracellular  $\text{Na}^+$ ,  $\text{Cl}^-$  or glycine are much lower than those of GlyT1b or that the forward and backward transport cycles do not have the same rate limiting step. Such transient release could be of physiological relevance because following synaptic release of glycine and its reuptake in neuron and glial cells, reverse transport by GlyT1b may occur if the extracellular concentration is driven too low by GlyT2 (Figure 7A).

To investigate the change in transport kinetics produced by glycine accumulation, oocytes were exposed continuously to a saturating glycine concentration (1 mM) for periods of up to 60 minutes, while the glycine-evoked current was monitored at different potentials every 40 s. The leak current measured before the application of glycine was subtracted from the total current. The evolution of  $I_T$  during and following a one hour glycine application (solid bar) from two representative experiments with GlyT1b<sup>+</sup> and GlyT2a<sup>+</sup> oocytes is plotted in figure 6D. For GlyT1b<sup>+</sup> oocytes, uptake currents recorded at  $V_H = -40$  mV (continuous line) fell dramatically as the glycine application was prolonged, approaching zero after 1 hour,

## Glycine transporters stoichiometries

suggesting that the transporter was close to equilibrium. In 5 experiments, a 50% reduction of  $I_T$  was observed after  $6.2 \pm 0.45$  minutes of glycine superfusion. As shown in the  $I_T$ - $V_m$ s of figure 6E, the decrease in inward current did not result from a change in the chord conductance but rather from a shift of the reversal potential toward more negative values. Upon removal of glycine, a larger driving force for reverse transport was present which produced an outward current that decreased progressively. In contrast, prolonged application of glycine on GlyT2a<sup>+</sup> oocytes did not produce a similar decrease of the inward current at negative potentials, indicating that the uptake capacity of GlyT2a was maintained (Figure 6D). At +40 mV,  $I_T$  became outward after ~15 minutes of glycine superfusion, allowing determination of the GlyT2a reversal potential. The  $I_T$ - $V_m$ s recorded at different times (Figure 6E) showed an increasing outward rectification with a progressive shift of  $E_{Rev}$  toward less positive values.

In figure 6F, GlyT1b and GlyT2a reversal potentials were plotted as a function of glycine uptake, estimated from the time integral of  $I_T$ . The mean values of  $E_{Rev}$  for 2 nmol of glycine uptake were  $+14.1 \pm 7.9$  mV ( $n = 12$ ) for GlyT1b and  $+37.1 \pm 1.6$  mV ( $n = 9$ ) for GlyT2a, indicating that GlyT2a was less sensitive to glycine accumulation, as expected for a higher stoichiometry. The glycine uptakes calculated from the time integral of  $I_T$  were similar with  $2.9 \pm .45$  ( $n = 2$ , GlyT1b) and  $2.4 \pm .1$  ( $n = 5$ , GlyT2a) nmol after 30 minutes of glycine incubation, despite the fact that in these experiments the apparent expression level of GlyT2a was only a quarter of that of GlyT1b (as indicated by their uptake current of 445 and 202 nA for GlyT1b and GlyT2a, respectively).

### Discussion

Despite their involvement in both inhibitory and excitatory transmission, the kinetics and energetics of glycine transporters have not been characterized as well as those of other neurotransmitter transporters. Here we report that the neuronal and glial glycine transporters have different stoichiometries and reverse transport capabilities. These differences correlate well with the hypothesis of specialized tasks for both transporters, suggested by their mRNA and protein localization (Smith et al., 1992; Liu et al., 1993; Zafra et al., 1995; Zafra et al., 1995): fast re-uptake of glycine into the pre-synaptic terminals for GlyT2a and control of the extracellular glycine concentration for GlyT1b.

### GlyT1b and GlyT2a Have Different Na<sup>+</sup> Stoichiometries

Simultaneous measurements of glycine-evoked current and glycine uptake reveal a major difference between the charge transferred per glycine of the neuronal and glial GlyTs. For GlyT1b, the charge to substrate flux ratio of +1 found between -120 and 0 mV matches what is expected from the “classical” 2 Na<sup>+</sup>/Cl<sup>-</sup>/glycine stoichiometry (Zafra and Gimenez, 1986; Aragon et al., 1987). In contrast, the excess charge found for GlyT2a ( $z_T \cong +2$ ) is not compatible with this stoichiometry. The additional charge does not result from an absence of net Cl<sup>-</sup> co-transport by GlyT2a, since both transporters have equal glycine and Cl<sup>-</sup> fluxes and that [Cl<sup>-</sup>]<sub>o</sub> affects the transporters reversal potentials. The fact that the extra charge is carried by a third Na<sup>+</sup> ion thermodynamically coupled to glycine uptake is further supported by three sets of observations on the  $E_{Rev}$  dependence on [Gly]<sub>o</sub>, [Gly]<sub>i</sub> and [Na<sup>+</sup>]<sub>o</sub>: 1) the transport reversal potentials were shifted by 61 mV for GlyT1b and 28.6 mV for GlyT2a for a tenfold change in [Gly]<sub>o</sub>, as expected from their difference in charge/glycine ratio; 2) the limited decrease of GlyT2a  $E_{Rev}$  observed during prolonged applications of

## Glycine transporters stoichiometries

glycine, compared to the large shift of GlyT1b  $E_{Rev}$ , is consistent with a lower sensitivity of  $E_T$  to a change in  $[Gly]_i$ ; 3) the variations of  $E_{Rev}$  for GlyT1b and GlyT2a as a function of  $[Na^+]_o$  agree with the predictions for  $n_{Na} = 2$  and  $n_{Na} = 3$ , respectively. Thus, we confirm that the classical stoichiometry of 2  $Na^+/Cl^-$ /glycine is correct for GlyT1b but conclude that for GlyT2a the stoichiometry is 3  $Na^+/Cl^-$ /glycine.

In the  $Na^+/Cl^-$ -coupled transporter family, the number of  $Na^+$  ions energetically coupled to the uptake of neurotransmitters appears to be variable, in contrast to the invariance of the  $Cl^-$  coupling ( $n_{Cl} = 1$ ) (Rudnick, 1998). The lowest coupling ( $n_{Na} = 1$ ) has been proposed for the norepinephrine (NET) and the serotonin transporters (SERT), with the additional counter-transport of one  $K^+$  or  $H^+$  ion in the latter case (reviewed in Rudnick, 1998). GlyT1b has the same  $Na^+$  coupling ( $n_{Na} = 2$ ) as the GABA transporter GAT1 (Radian and Kanner, 1983; Mager et al., 1993; Lu and Hilgemann, 1999) and the dopamine transporter (DAT) (Sonders et al., 1997). GlyT2a is the first member of this family found to be coupled to 3  $Na^+$ . In the glutamate transporter family, studies using a similar methodology have reported the same 3  $Na^+$  stoichiometry for the neuronal EAAT3 (Zerangue and Kavanaugh, 1996) and glial GLT1 (Levy et al., 1998) transporters. However, despite their identical stoichiometries, these two glutamate transporters do not accumulate similar intracellular/extracellular gradients in neurons and astrocytes where glutamate is converted to glutamine (reviewed in Kanai, 1997). This suggests that under physiological conditions, a transporter may not reach equilibrium, as a balance is achieved between the size of the concentration gradient and the capacity to maintain a high uptake rate. Under non-equilibrium conditions, the greater driving force of GlyT2a may allow it to compete effectively with GlyT1b for glycine released at the synapse, despite the higher intracellular glycine concentration.

## Glycine transporters stoichiometries

Estimates of the glycine concentration ratios ( $[Gly]_i / [Gly]_o$ ) that GlyT1b and GlyT2a can maintain at equilibrium are  $\sim 3 \cdot 10^4$  and  $4 \cdot 10^6$  respectively, taking  $[Na^+]_o = 145$  mM,  $[Na^+]_i = 14$  mM,  $[Cl^-]_o = 120$  mM,  $[Cl^-]_i = 6$  mM and  $V_m = -70$  mV at 37 °C. Assuming that intracellular glycine is 2 mM in astrocytes (in the hippocampus, Berger et al., 1977) and 10 mM in glycinergic neurons (Ottersen et al., 1990), these ratios are compatible with an extracellular glycine concentration below 0.1  $\mu$ M, which is below saturation for NMDARs (see Figure 7A). During ischemia, the accumulating power of GlyT1b falls below  $10^2$  (assuming  $[Na^+]_o = 85$  mM,  $[Na^+]_i = 25$  mM,  $[Cl^-]_o = 120$  mM,  $[Cl^-]_i = 35$  mM,  $V_m = -20$  mV), which gives a minimal extracellular concentration of 20  $\mu$ M, close to what has been measured (Baker et al., 1991).

The difference in  $Na^+$  stoichiometry may be the basis of most of the kinetic differences existing between the steady-state and pre steady-state currents of the two glycine transporters. Thus, the equivalent charge corresponding to the voltage-dependencies of the apparent  $Na^+$  and glycine affinities are higher for GlyT2a than for GlyT1b. Differences in the characteristic transient currents observed in the absence of glycine but in the presence of  $Na^+$  also provide good support for binding of more  $Na^+$  ions to GlyT2a compared to GlyT1b (manuscript in preparation).

### **Tight Coupling Between Uptake and Glycine-Evoked Current**

The proportionality between glycine uptake and glycine-evoked current over a wide range of potentials is of particular importance for the analysis of the roles of glycine transporters, as it means that glycine uptake can be monitored with the high time resolution of electrophysiological techniques. The fact that this proportionality is that expected from the transport stoichiometry contrasts with recent electrophysiological characterization of neurotransmitter transporters, which have established uncoupled

## Glycine transporters stoichiometries

currents as a rule rather than an exception. SERT, NET, GAT, DAT and EAATs have been reported to have higher substrate-evoked currents than expected from their transport stoichiometry (reviewed in Sonders and Amara, 1996). However, two remarks should be made. First, EAATs stand apart, as the main charge carrier of their uncoupled current is  $\text{Cl}^-$  which is not a substrate for these transporters. Second, the monoamine transporters face a smaller gradient than the other transporters, as monoamine oxidase keeps the intracellular concentrations of their substrates in the micromolar range, while GAT, EAATs, GlyTs and the  $\text{Na}^+$  / glucose cotransporter SGLT1 must face millimolar intracellular concentrations of their substrates, 3 orders of magnitude higher than those of monoamines.

Large charge to substrate fluxes ratio (3 to 200 charges per substrate molecule) have been reported consistently only for the monoamine transporters (reviewed in Sonders and Amara, 1996; see also Galli et al., 1997; Sonders et al., 1997). Contrasting with these results, between +1 and +2 charges per glutamate were found for EAAT1-3 in absence of the uncoupled but permeant anion  $\text{Cl}^-$  (Wadiche et al., 1995; Zerangue and Kavanaugh, 1996) and the  $^{22}\text{Na}^+$  to glucose flux ratio of SGLT1 was found to be close to +2 (Mackenzie et al., 1998). GlyTs behave in the same way, with a tight coupling between ionic and substrate fluxes. This is particularly true for GlyT1b, which exhibits no leak current and has a strictly voltage-independent  $z_T$ . The charge coupling of GlyT2a appears less tight, but the observed variations of  $z_T$  are quite small (0.4 charges between  $-120$  mV and  $0$  mV) compared to other transporters.

### **Differences in Glycine Efflux**

The thermodynamics of ion-coupled transport impose that transporters work in a reverse mode when the membrane potential is more positive than their equilibrium

## Glycine transporters stoichiometries

potential. This inversion is well explained by cyclic alternative access models (Lu and Hilgemann, 1999). Experimental evidence for non vesicular, calcium-independent liberation of neurotransmitters has been reported for GABA and glutamate transporters, and reverse uptake is supposed to be a major release mechanism of GABA by retinal horizontal cells or for glutamate during ischemia (see review in Attwell et al., 1993).

Here, we show that GlyT2a has a kinetic constraint for reverse transport that limits glycine release. Such asymmetry in glycine fluxes may be essential to maintain a high content of neurotransmitter inside the pre-synaptic neurons during periods of electrical activity. However, it has not been found for other neuronal transporters such as EAAT3 (Zerangue and Kavanaugh, 1996; Levy et al., 1998) and GAT1 (Cammack et al., 1994; Lu and Hilgemann, 1999).

In our experimental conditions, GlyT reverse transport was not detected unless intracellular glycine, Na<sup>+</sup> or Cl<sup>-</sup> concentrations were elevated by microinjection or prolonged uptake, producing outward currents that could be blocked by transporter inhibitors as described in figure 4. The difference in the voltage-dependence of GlyT2a inward and outward currents (Figure 5B) implies that the forward and backward cycles are not governed by the same kinetic steps, the nature of which has not been precisely determined. Decreasing the external Na<sup>+</sup> or glycine concentrations did not enhance outward currents, which suggests that external unbinding of ligands is not limiting. In contrast, internal binding of Na<sup>+</sup> to the transporter may be critical, since microinjection of glycine alone failed to activate outward current with GlyT2a despite the decrease of the reversal potential (Figure 4B, top trace). This suggests that the third intracellular Na<sup>+</sup> site has a lower affinity that limits reverse transport.

## Glycine transporters stoichiometries

In contrast, the fact that GlyT1b exhibits no such limitation for reverse transport could be appropriate at both excitatory and inhibitory synapses as illustrated in figure 7B. Near glycinergic terminals, the difference in energetic coupling of the two transporters may allow some leak of glycine from astrocytes by reverse transport that could subsequently be pumped by GlyT2a into neurons. At glutamatergic synapses, GlyT1b will lower ambient glycine to a submicromolar concentration thus reducing NMDAR activation through their high-affinity glycine modulatory site (Supplisson and Bergman, 1997; Berger et al., 1998; Bergeron et al., 1998).

Attwell et al. (1993) have suggested that activation of AMPARs in glial cells by glutamate may produce a depolarization and a rise in  $[Na^+]_i$  that could be sufficient to reverse GlyT1b transport thus increasing the  $[Gly]_o$  and potentiating NMDA receptors (Figure 7B). In support of this model, AMPARs and transporter currents activated by synaptic release of glutamate have been recorded *in situ* from Bergmann cells in the cerebellum, after stimulation of the parallel fibers (Clark and Barbour, 1997) or the climbing fibers (Bergles et al., 1997). In hippocampal slices, stimulation of the Schaffer collateral evoked AMPARs and transporter currents in CA1 astrocytes (Diamond et al., 1998; Lüscher et al., 1998). The resulting depolarization and change in  $[Na^+]_i$  (which could be significant because of the low intracellular volume of fine astroglial process) may be sufficient to reverse locally GlyT1b.

## Experimental Procedures

### Transporters Expression in *Xenopus* Oocytes

Rat GlyT1b (gift from K. Smith, Synaptic Corporation (Smith et al., 1992)) and rat GlyT2a (gift from B. López-Corcuera and C. Aragón (Liu et al., 1993) cDNAs were subcloned as indicated in Supplisson and Bergman, 1997. cRNAs were transcribed *in vitro* using the T7 mMessage-mMachine kit (Ambion) and 10-100ng were injected into oocytes using a nanoliter injector (World Precision Instruments).

Defolliculated oocytes were isolated from *Xenopus laevis* ovaries after 1 hour of shaking incubation in OR-2 Ca<sup>2+</sup>-free medium containing 2 mg.ml<sup>-1</sup> of collagenase type II (GIBCO). Oocytes were kept at 19°C in individual wells containing 200 µl of Barth solution (88 mM NaCl, 1 mM KCl, 2.4 mM NaHCO<sub>3</sub>, 0.82 mM MgSO<sub>4</sub>, 0.33 mM Ca(NO<sub>3</sub>)<sub>2</sub>, 0.41 mM CaCl<sub>2</sub>, 10 mM HEPES, pH 7.4 adjusted with NaOH, 50 µg/ml of gentamycin). Experiments were performed at room temperature (19-24°C), 3 to 15 days after cRNA injection.

Samples of glycine inhibitors were generously provided by Glenn Walker (ORG24958) and Hardy Sudaram (ORG26176) (David Hill, Organon, Scotland, UK).

### Electrophysiology and Data Analysis

For most experiments whole-cell currents were recorded as described in Supplisson and Bergman, 1997. For uptake experiments, an open Teflon® chamber was used, with a 3 M K-gluconate agar bridge when required. The typical extracellular recording solution contained (in mM): 100 NaCl, 1.8 CaCl<sub>2</sub>, 1 MgCl<sub>2</sub>, 5 HEPES, pH 7.2 adjusted with KOH. In some experiments, choline and gluconate were substituted for Na<sup>+</sup> and Cl<sup>-</sup>, respectively. Salts and glycine were purchased from SIGMA. Data are given as mean ± S.E.M. with the number of experiments.

### **Uptake Assays**

Glycine uptake: GlyT1b<sup>+</sup> or Glyt2a<sup>+</sup> oocytes were voltage-clamped at different holding potentials (from 0 to -120 mV) and after application of 25  $\mu$ M of U-<sup>14</sup>C glycine (Specific Activity of 103 mC/mmol, Amersham) for 45 to 120 seconds, oocytes were superfused for 30 to 60 seconds in control Ringer solution, then promptly washed in 1 ml ice-cold choline-Cl Ringer for 10 seconds.

Chloride uptake: oocytes were hold at -30 mV and superfused with a 90 mM Na gluconate / 10 mM NaCl solution until stabilization of the membrane current (3 to 15 min), then superfused for 30 to 50 seconds with a 90 mM Na gluconate / 10 mM Na <sup>36</sup>Cl (Specific Activity of ~0.5 mC/mmol, Amersham) solution containing 1 mM glycine. The solution flow was stopped for 4 to 14 minutes, then oocytes were superfused with the initial 10 mM NaCl solution for 1-2 minutes, promptly washed three times in ice-cold choline-Cl Ringer, put in solution containing 0.5 ml of 1% SDS and counted on a Kontron Betamatic.

### **Acknowledgments**

We are grateful to Philippe Ascher for his encouragement, support and invaluable comments on the manuscript. Thanks to Boris Barbour for critically reading and comments on the manuscript; to Stéphane Dieudonné, Baruch Kanner and Donald F. Loo for stimulating discussions; and to Anne Le Goff for technical assistance. This work was supported by the CNRS and a grant from the European Community (contract BMH4CT950571).

## References

- Adams, R. H., Sato, K., Shimada, S., Tohyama, M., Puschel, A. W., and Betz, H. (1995). Gene structure and glial expression of the glycine transporter GlyT1 in embryonic and adult rodents. *J Neurosci* 15, 2524-2532.
- Aprison, M. H., and Werman, R. (1965). The distribution of glycine in cat spinal cord and roots. *Life Sci* 4, 2075-2083.
- Aragon, M. C., Gimenez, C., and Mayor, F. (1987). Stoichiometry of sodium- and chloride-coupled glycine transport in synaptic plasma membrane vesicles derived from rat brain. *FEBS Lett* 212, 87-90.
- Ascher, P. (1990). Measuring and controlling the extracellular glycine concentration at the NMDA receptor level. *Exp. Med. Biol Adv.* 268, 13-16.
- Attwell, D., Barbour, B., and Szatkowski, M. (1993). Non vesicular release of neurotransmitter. *Neuron* 11, 401-407.
- Baker, A. J., Zornow, M. H., Scheller, M. S., Yaksh, T. L., Skilling, S. R., Smullin, D. H., Larson, A. A., and Kuczenski, R. (1991). Changes in extracellular concentrations of glutamate, aspartate, glycine, dopamine, serotonin, and dopamine metabolites after transient global ischemia in the rabbit brain. *J Neurochem* 57, 1370-1379.
- Berger, A. J., Dieudonne, S., and Ascher, P. (1998). Glycine uptake governs glycine site occupancy at NMDA receptors of excitatory synapses. *J Neurophysiol* 80, 3336-3340.
- Berger, S. J., Carter, J. C., and Lowry, O. H. (1977). The distribution of glycine, GABA, glutamate and aspartate in rabbit spinal cord, cerebellum and hippocampus. *J Neurochem* 28, 149-158.
- Bergeron, R., Meyer, T. M., Coyle, J. T., and Greene, R. W. (1998). Modulation of N-methyl-D-aspartate receptor function by glycine transport. *Proc Natl Acad Sci U S A* 95, 15730-15734.
- Bergles, D. E., Diamond, J. S., and Jahr, C. E. (1999). Clearance of glutamate inside the synapse and beyond. *Curr Opin Neurobiol* 9, 293-298.
- Bergles, D. E., Dzubay, J. A., and Jahr, C. E. (1997). Glutamate transporter currents in bergmann glial cells follow the time course of extrasynaptic glutamate. *Proc Natl Acad Sci U S A* 94, 14821-14825.
- Borowsky, B., and Hoffman, B. J. (1998). Analysis of a gene encoding two glycine transporter variants reveals alternative promoter usage and a novel gene structure. *J Biol Chem* 273, 29077-29085.
- Cammack, J. N., Rakhilin, S. V., and Schwartz, E. A. (1994). A GABA transporter operates asymmetrically and with variable stoichiometry. *Neuron* 13, 949-960.

## Glycine transporters stoichiometries

- Clark, B. A., and Barbour, B. (1997). Currents evoked in Bergmann glial cells by parallel fibre stimulation in rat cerebellar slices. *J Physiol (Lond)* 502, 335-350.
- Danysz, W., and Parsons, A. C. G. (1998). Glycine and N-methyl-D-aspartate receptors: physiological significance and possible therapeutic applications. *Pharmacol Rev* 50, 597-664.
- Diamond, J. S., Bergles, D. E., and Jahr, C. E. (1998). Glutamate release monitored with astrocyte transporter currents during LTP. *Neuron* 21, 425-433.
- Fern, R., Connolly, G. P., and Harrison, P. J. (1996). Evidence for functional co-activation of N-methyl-D-aspartate receptors by glycine. *Neuroreport* 7, 1953-1956.
- Galli, A., Petersen, C. I., deBlaquiere, M., Blakely, R. D., and DeFelice, L. J. (1997). Drosophila serotonin transporters have voltage-dependent uptake coupled to a serotonin-gated ion channel. *J Neurosci* 17, 3401-3411.
- Grenningloh, G., Rienitz, A., Schmitt, B., Methfessel, C., Zensen, M., Beyreuther, K., Gundelfinger, E. D., and Betz, H. (1987). The strychnine-binding subunit of the glycine receptor shows homology with nicotinic acetylcholine receptors. *Nature* 328, 215-220.
- Johnson, J. W., and Ascher, P. (1987). Glycine potentiates the NMDA response in cultured mouse brain neurons. *Nature* 325, 529-531.
- Jursky, F., and Nelson, N. (1995). Localization of glycine neurotransmitter transporter (GLYT2) reveals correlation with the distribution of glycine receptor. *J Neurochem* 64, 1026-1033.
- Kanai, Y. (1997). Family of neutral and acidic amino acid transporters: molecular biology, physiology and medical implications. *Curr Opin Cell Biol* 9, 565-572.
- Kanner, B. I., and Schuldiner, S. (1987). Mechanism of transport and storage of neurotransmitters. *CRC Critical Reviews in Biochemistry* 22, 1-38.
- Levy, L. M., Warr, O., and Attwell, D. (1998). Stoichiometry of the glial glutamate transporter GLT-1 expressed inducibly in a Chinese hamster ovary cell line selected for low endogenous Na<sup>+</sup>-dependent glutamate uptake. *J Neurosci* 18, 9620-9628.
- Liu, Q. R., Lopez-Corcuera, B., Mandiyan, S., Nelson, H., and Nelson, N. (1993). Cloning and expression of a spinal cord- and brain-specific glycine transporter with novel structural features. *J. Biol. Chem.* 268, 22802-22808.
- Loo, D. D., Hazama, A., Supplisson, S., Turk, E., and Wright, E. M. (1993). Relaxation kinetics of the Na<sup>+</sup>/glucose cotransporter. *Proc. natl. Acad. Sci. U.S.A* 90, 5767-5771.
- Lu, C. C., and Hilgemann, D. W. (1999). GAT1 (GABA:Na<sup>(+)</sup>:Cl<sup>(-)</sup>) Cotransport Function. Steady state studies in giant xenopus oocyte membrane patches. *J Gen Physiol* 114, 429-444.
- Luque, J. M., Nelson, N., and Richards, J. G. (1995). Cellular expression of glycine

## Glycine transporters stoichiometries

transporter 2 messenger RNA exclusively in rat hindbrain and spinal cord. *Neurosci* 64, 525-535.

Lüscher, C., Malenka, R. C., and Nicoll, R. A. (1998). Monitoring glutamate release during LTP with glial transporter currents. *Neuron* 21, 435-441.

Mackenzie, B., Loo, D. D., and Wright, E. M. (1998). Relationships between Na<sup>+</sup>/glucose cotransporter (SGLT1) currents and fluxes. *J Membr Biol* 162, 101-106.

Mager, S., Naeve, J., Quick, M., Labarca, C., Davidson, N., and Lester, H. A. (1993). Steady states, charge movements, and rates for a cloned GABA transporter expressed in *Xenopus* oocytes. *Neuron* 10, 177-188.

Ottersen, O. P., Storm-Mathisen, J., Bramham, C., Torp, R., Laake, J., and Gundersen, V. (1990). A quantitative electron microscopic immunocytochemical study of the distribution and synaptic handling of glutamate in rat hippocampus. *Prog Brain Res* 83, 99-114.

Palacin, M., Estevez, R., Bertran, J., and Zorzano, A. (1998). Molecular biology of mammalian plasma membrane amino acid transporters. *Physiol Rev* 78, 969-1054.

Poyatos, I., Ponce, J., Aragon, C., Gimenez, C., and Zafra, F. (1997). The glycine transporter GLYT2 is a reliable marker for glycine-immunoreactive neurons. *Brain Res Mol Brain Res* 49, 63-70.

Radian, R., and Kanner, B. I. (1983). Stoichiometry of sodium- and chloride-coupled gamma-aminobutyric acid transport by synaptic plasma membrane vesicles isolated from rat brain. *Biochemistry* 22, 1236-1241.

Rudnick, G. (1998). Bioenergetics of neurotransmitter transport. *J Bioenerg Biomembr* 30, 173-185.

Sagne, C., El Mestikawy, S., Isambert, M. F., Hamon, M., Henry, J. P., Giros, B., and Gasnier, B. (1997). Cloning of a functional vesicular GABA and glycine transporter by screening of genome databases. *FEBS Lett* 417, 177-183.

Singer, J. H., and Berger, A. J. (1999). Contribution of single-channel properties to the time course and amplitude variance of quantal glycine currents recorded in rat motoneurons. *J Neurophysiol* 81, 1608-1616.

Smith, K. E., Borden, L. A., Hartig, P. R., Branchek, T., and Weinshank, R. L. (1992). Cloning and expression of a glycine transporter reveal colocalization with NMDA receptors. *Neuron* 8, 927-935.

Sonders, M. S., and Amara, S. G. (1996). Channels in transporters. *Curr Opin Neurobiol* 6, 294-302.

Sonders, M. S., Zhu, S. J., Zahniser, N. R., Kavanaugh, M. P., and Amara, S. G. (1997). Multiple ionic conductances of the human dopamine transporter: the actions of dopamine and psychostimulants. *J Neurosci* 17, 960-974.

Spike, R. C., Watt, C., Zafra, F., and Todd, A. J. (1997). An ultrastructural study of

## Glycine transporters stoichiometries

the glycine transporter GLYT2 and its association with glycine in the superficial laminae of the rat spinal dorsal horn. *Neuroscience* 77, 543-551.

Storm-Mathisen, J., and Ottersen, O. P. (1990). Cellular and subcellular localization of glycine studied by quantitative electron microscopic immunocytochemistry. *Glycine Neurotransmission*, 303-328.

Supplisson, S., and Bergman, C. (1997). Control of NMDA receptor activation by a glycine transporter co- expressed in *Xenopus* oocytes. *J Neurosci* 17, 4580-4590.

Titmus, M. J., Korn, H., and Faber, D. S. (1996). Diffusion, not uptake, limits glycine concentration in the synaptic cleft. *J Neurophysiol* 75, 1738-1752.

Wadiche, J. I., Amara, S. G., and Kavanaugh, M. P. (1995). Ion fluxes associated with excitatory amino acid transport. *Neuron* 15, 721-728.

Walker, G., Morrow, J., Hamilton, W., Bruin, J., Shadid, M., Stam, N., and Hill, D. (1999). In vitro characterisation of ORG 24598, a selective glycine uptake inhibitor. *Soc. Neurosci. Abstract* 25, 165.

Zafra, F., Aragon, C., and Gimenez, C. (1997). Molecular biology of glycinergic neurotransmission. *Mol Neurobiol* 14, 117-142.

Zafra, F., Aragon, C., Olivares, L., Danbolt, N. C., Gimenez, C., and Storm-Mathisen, J. (1995). Glycine transporters are differentially expressed among CNS cells. *J Neurosci* 15, 3952-3969.

Zafra, F., and Gimenez, C. (1986). Characterization of glycine uptake in plasma membrane vesicles isolated from cultured glioblastoma cells. *Brain Res* 397, 108-116.

Zafra, F., Gomeza, J., Olivares, L., Aragon, C., and Gimenez, C. (1995). Regional distribution and developmental variation of the glycine transporters GLYT1 and GLYT2 in the rat CNS. *Eur J Neurosci* 7, 1342-1352.

Zerangue, N., and Kavanaugh, M. P. (1996). Flux coupling in a neuronal glutamate transporter. *Nature* 383, 634-637.

## Figure Legends

### Figure 1. Charge coupling of GlyT1b and GlyT2a

Comparison of U-<sup>14</sup>C glycine (A-C) or <sup>36</sup>Cl (D) uptake with the time integral of the glycine-evoked currents recorded under voltage-clamp.

(A-B) Current response evoked by 25  $\mu$ M <sup>14</sup>C glycine (solid bar) in control Ringer or when Na<sup>+</sup> or Cl<sup>-</sup> was replaced by choline or gluconate, respectively. Holding potential was -80 mV. In Na<sup>+</sup>-free solution, application of 25  $\mu$ M U-<sup>14</sup>C glycine during 1 to 2 minutes produced the same uptake in GlyT1b<sup>+</sup> oocytes ( $0.51 \pm 0.19$  pmol, n = 3) as in non-injected oocytes ( $0.56 \pm 0.36$  pmol, n = 4). Similar "baseline" values were observed in Cl<sup>-</sup>-free solutions for GlyT1b ( $0.55 \pm 0.15$  pmol, n = 3) but were slightly higher for GlyT2a ( $1.53 \pm 0.7$  pmol, n = 3).

(C) Time integrals of glycine-evoked currents (shaded in gray in A and B), expressed in pmol of elementary charges, plotted as a function of glycine uptake for GlyT1b<sup>+</sup> (n = 19) and GlyT2a<sup>+</sup> (n = 18) oocytes at various potentials. Glycine applications varied between 45 and 120 s.

(D) <sup>36</sup>Cl uptake is plotted as a function of the equivalent glycine uptake estimated from the time integrals of glycine-evoked currents (shaded in gray in A-B) using their specific charge to glycine flux ratios. GlyT1b<sup>+</sup> (n = 8) and GlyT2a<sup>+</sup> (n = 17) oocytes were pre-equilibrated in a solution containing 90 mM Na-gluconate and 10 mM NaCl before application of 500  $\mu$ M glycine in a Ringer solution containing 10 mM Na <sup>36</sup>Cl and 90 mM Na-gluconate. The holding potential was -30 mV.

### Figure 2. Relaxation and uptake currents of GlyT1b and GlyT2a

(A and B) A representative GlyT1b<sup>+</sup> oocyte was held at -40 mV and the potential

## Glycine transporters stoichiometries

was stepped to values ranging from +40 mV to -160 mV (20 mV decrements), in the absence (A) or in the presence of 200  $\mu$ M glycine (B).

(C) I-V relationships of the steady-state currents recorded in A and B (see corresponding symbols).

(D) I-V relationship of the glycine-evoked current.

(E and F) A representative GlyT2a<sup>+</sup> oocyte was held at -40 mV and the potential was stepped to values ranging from +40 mV to -140 mV (20 mV decrements), in the absence (E) or in the presence of 1 mM glycine (F).

(G) I-V relationships of the steady-state currents of A and B (see corresponding symbols).

(H) I-V relationship of the steady-state glycine-evoked current.

In A-B and E-F the dashed line indicates the zero-current level and the first 1.75 ms after each voltage jump were omitted for clarity. In D and H, the conductance corresponds to the linear regression of the current values between -110 and -70 mV (dashed line).

### Figure 3. Apparent affinities of glycine transporters for Na<sup>+</sup> and glycine

Glycine-evoked currents of GlyT1b and GlyT2a were measured as described in figure 2 for various [Gly]<sub>o</sub> or [Na<sup>+</sup>]<sub>o</sub>. Values superior to -5 nA were discarded.

(A-B) Dose-response curves for glycine concentrations between 2  $\mu$ M and 3 mM (GlyT1b, A) or between 1  $\mu$ M and 2 mM (GlyT2a, B), for membrane potentials between +50 mV and -130 mV. Solid lines represent fits to the data using a

Michaelis-Menten equation  $I_{TG}^{Gly} = I_{TG\max}^{Gly} / \{1 + K_{0.5}^{Gly} / [Gly]\}$ .

(C) Voltage-dependence of the apparent glycine affinity  $K_{0.5}^{Gly}$ . Solid lines are fits to

## Glycine transporters stoichiometries

the data using the phenomenological equation  $K_{0.5}^{Gly} = A + B e^{(-z\delta_{Gly} V_m F / RT)}$ .

(D-E) Dose-response curves for  $\text{Na}^+$  concentrations between 1 and 100 mM (GlyT1b, D) or between 2 and 100 mM (GlyT2a, E), for membrane potentials between +30 mV and -130 mV. Solid lines represent fits to the data using a Hill equation

$$I_{TG}^{Na} = I_{TG\max}^{Na} / \left\{ 1 + (K_{0.5}^{Na} / [\text{Na}^+])^{n_{Na}} \right\}. \text{ Values over +20 mV were not fitted.}$$

(F) Voltage-dependence of the apparent  $\text{Na}^+$  affinity  $K_{0.5}^{Na}$ . Solid lines are fit to the data using the phenomenological equation  $K_{0.5}^{Na} = A + B e^{(-z\delta_{Na} V_m F / RT)}$ .

(G) Hill coefficients ( $n_{Na}$ ) as determined in D and E. The dashed line corresponds to  $n_{Na} = 2$ .

### **Figure 4. Microinjection of $\text{Na}^+$ and glycine evoked outward currents in GlyT1b<sup>+</sup> and GlyT2a<sup>+</sup> oocytes.**

(A-B) Current traces showing the activation of outward currents and / or diminution of inward glycine-evoked current after intracellular injection (vertical bars and indicated by arrows) of 16 nmol of glycine for GlyT1b (A) and GlyT2a (B, top trace) or glycine and NaCl for GlyT2a (B, bottom trace). Glycine (100  $\mu\text{M}$ , black bar) was superfused before and after intracellular injection. Application of 10  $\mu\text{M}$  of the GlyT1 inhibitor ORG24598 (A) or 5  $\mu\text{M}$  of the GlyT2 inhibitor ORG26176 (B) (gray bar) blocked both inward and outward transporters currents ( $V_H = -40\text{mV}$ ). The dashed line represents the current level in the presence of inhibitor.

(C) Diagram of the experimental protocol. The oocytes were impaled with a third pipette connected to a nanoliter injector (WPI) and filled with a concentrated (1 M) solution of either glycine or glycine and NaCl. The estimated increase in  $[\text{Gly}]_i$ ,  $[\text{Na}^+]_i$ , and  $[\text{Cl}^-]_i$  for a maximal 16 nanoliters injection is  $\sim 30$  mM, modeling the oocyte as a 1

mm diameter sphere.

**Figure 5. Na<sup>+</sup>-dependence of transport reversal potential confirms the difference in stoichiometry between GlyT1b and GlyT2a**

(A-B) GlyT1b<sup>+</sup> oocytes were injected with 16 nmol of glycine (A) while GlyT2a<sup>+</sup> oocytes were injected with 16 nmol of glycine and NaCl (B). Following injection, oocytes were superfused with 100 μM glycine solutions containing different Na<sup>+</sup> concentrations (choline substitution). Transport currents were isolated from leak currents by subtraction of currents measured in the presence of 10 μM of the transporter inhibitor ORG24598 for GlyT1b (A) or 5 μM of the transporter inhibitor ORG26176 for GlyT2a (B).

(C-D) GlyT1b (C) and GlyT2a (D) reversal potentials are plotted as a function of the external Na<sup>+</sup> concentration after injection of 16 nmol of glycine (GlyT1b, n = 10) or glycine and NaCl (GlyT2a, n = 7). The solid line is a fit of the data with a logarithmic equation.

**Figure 6. Difference in outward current following glycine uptake**

(A) GlyT1b (○) and GlyT2a (●) steady-state currents were monitored every 30 s before and after a 1 minute application of 1 mM glycine (solid bar) using voltage-steps protocols as in figure 2. Values for potentials between -70 mV and +30 mV are plotted as a function of time ( $V_H = -40$  mV).

(B) Difference ( $I_2 - I_1$ ) in the steady-state current amplitudes before ( $I_1$ ) and just after ( $I_2$ ) a 2.6 minutes application of 1 mM glycine (n = 15 and n = 8 for GlyT1b (○) and GlyT2a (●), respectively). The solid line corresponds to a fit to  $I = I_0 e^{(-z\delta V_m F / RT)}$  with  $z\delta = 0.52 \pm 0.05$  (n = 15, S.D.).

(C) Relation between glycine uptake (estimated from the time integral of the glycine-

## Glycine transporters stoichiometries

evoked current) and the current difference ( $I_2 - I_1$ ) for GlyT1b (○) and GlyT2a (●). Solid lines are linear regression fits to the data. Two values obtained from GlyT1b<sup>+</sup> oocytes for which the leak increased during the experiment are also plotted (◇).

(D) GlyT1b (top) and GlyT2a (bottom) steady-state currents were monitored every 40 s using voltage-steps protocols as above, prior, during and after a one hour application of 1 mM glycine (solid bar). During this experiment, the oocyte was held 91% of the time at -40 mV. Evolution of the current is shown for potentials of -100 mV (gray circles), -40 mV (solid line) and +40 mV (open circles).

(E) Current-voltage relation of GlyT1b (top, open symbols) and GlyT2a (bottom, closed symbols) for different 1mM glycine application duration: 5 s (□, ■), 5 min (○, ●), 10 min (△, ▲), 20 min (◇, ◆), 30 min (▽, ▼) and 40 min, 50 min and 60 min (solid lines).

(F) Evolution of the reversal potential as a function of the glycine uptake for the same oocytes as in panels D and E, estimated from the time-integrals of the glycine-evoked currents (GlyT1b ○, and GlyT2a, ●). Mean values of  $E_{Rev}$  for 2 nmol glycine uptake and mean values of glycine uptake for  $E_{Rev} = +20\text{mV}$  are indicated ( $n = 12$  and  $n = 9$  for GlyT1b (◇) and GlyT2a (◆), respectively).

### Figure 7. Complementary roles of glycine transporters

(A) GlyT1b (thin line) and GlyT2a (thick line) equilibrium potentials as a function of the external glycine concentration, assuming  $[\text{Na}^+]_o = 145 \text{ mM}$ ,  $[\text{Na}^+]_i = 14 \text{ mM}$ ,  $[\text{Cl}^-]_o = 120 \text{ mM}$ ,  $[\text{Cl}^-]_i = 6 \text{ mM}$ ,  $37 \text{ }^\circ\text{C}$ , and glial and neuronal intracellular glycine concentrations of 2 mM and 10 mM, respectively. Reverse transport conditions are shaded in gray. For a resting potential of -70 mV (thin dotted line), GlyT1b is close to equilibrium for  $[\text{Gly}]_o = 100 \text{ nM}$  while the driving force for uptake by GlyT2a is still 50

## Glycine transporters stoichiometries

mV at this external concentration, which could lead to a kinetic advantage of GlyT2a over GlyT1b.

(B) At glycinergic synapses (left), glycine is removed from the extracellular space by complementary activity of the neuronal GlyT2a and GlyT1b found on the neighboring astrocyte processes. If, due to GlyT2a activity,  $[Gly]_o$  falls below the GlyT1b equilibrium value, these transporters will then work backwards, letting glycine leak out from astrocytes to be subsequently pumped back into neurons by GlyT2a. At glutamatergic synapses, GlyT1b uptake should maintain  $[Gly]_o$  beneath the saturation level of the NMDARs glycine site. However, activation of glial AMPARs by glutamate can lead to reverse transport conditions by depolarizing the astrocytes and raising  $[Na^+]_i$  locally, thus enhancing NMDAR responses. High activity of neighboring glycinergic synapses could also increase  $[Gly]_o$  at glutamatergic synapses, either by neurotransmitter spill-over or local reverse transport by GlyT1b following uptake of glycine in astrocyte processes close to the inhibitory synapses.

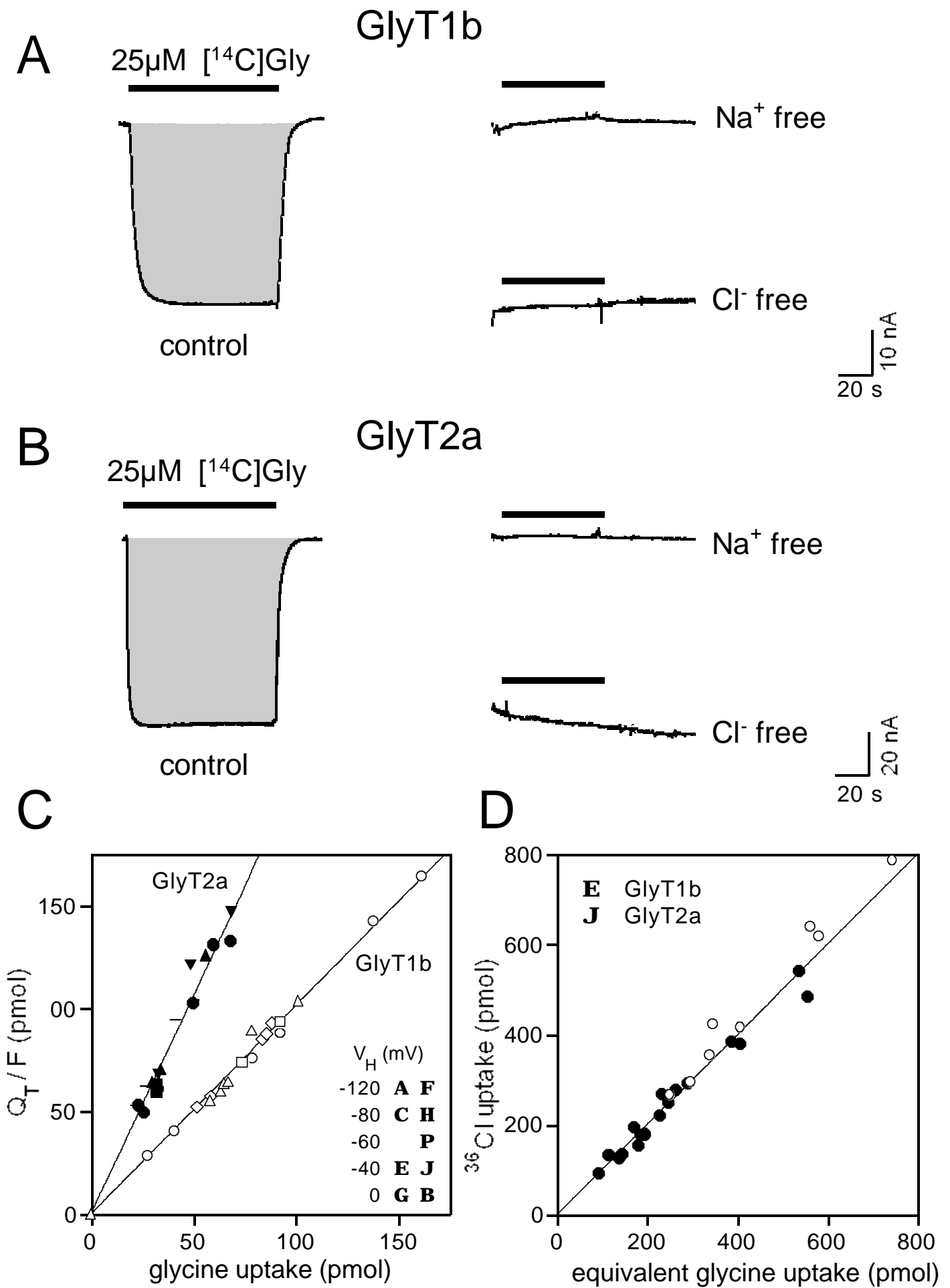


Figure 1

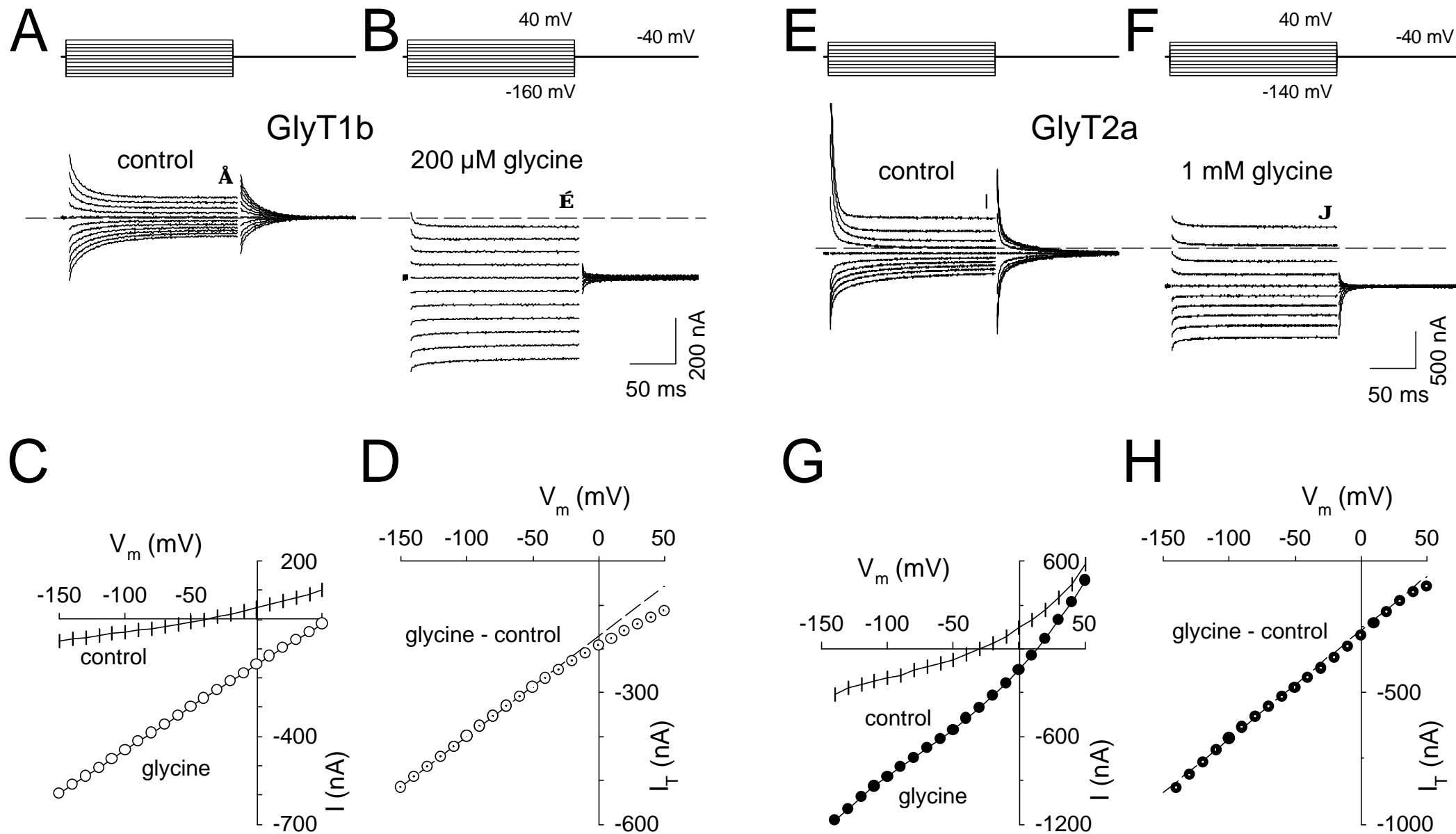
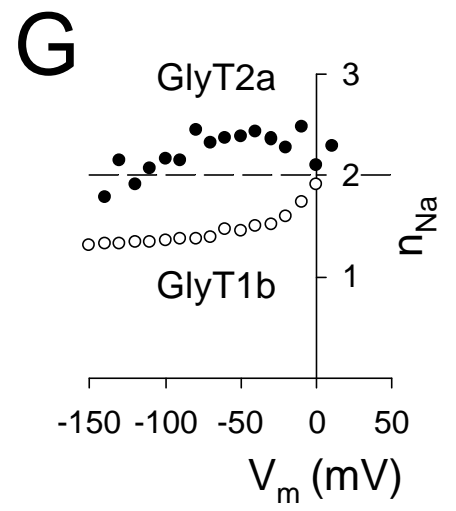
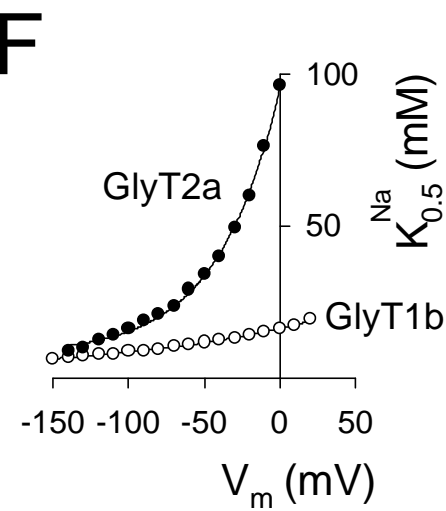
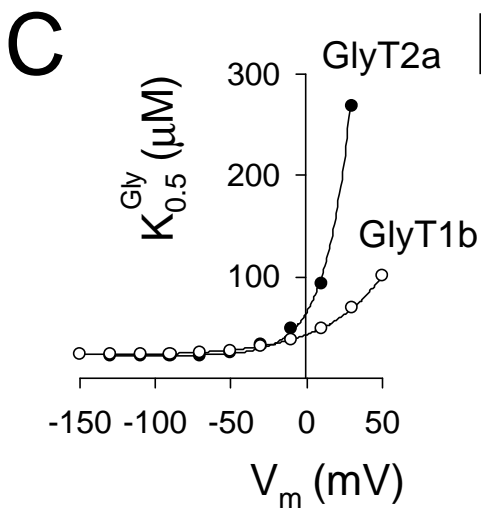
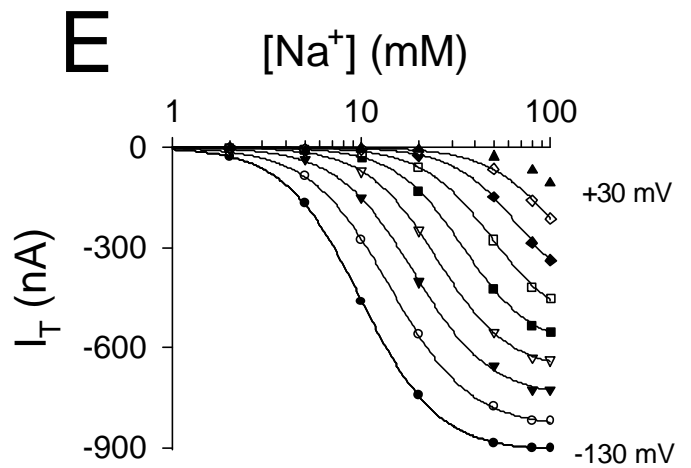
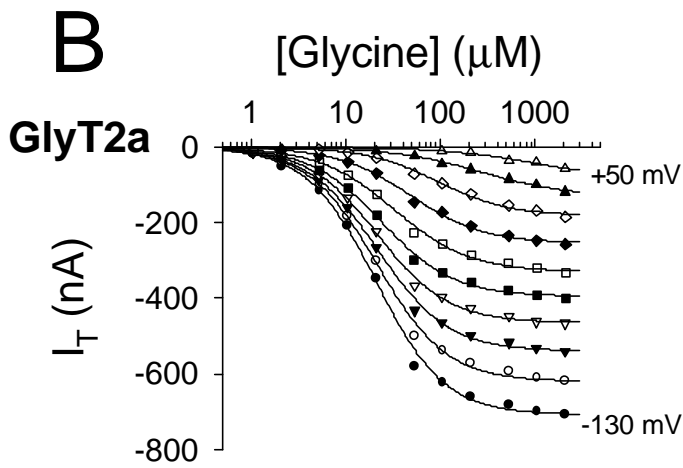
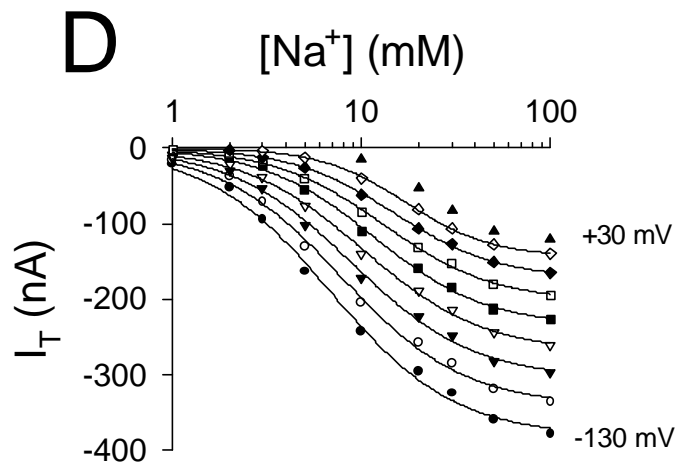
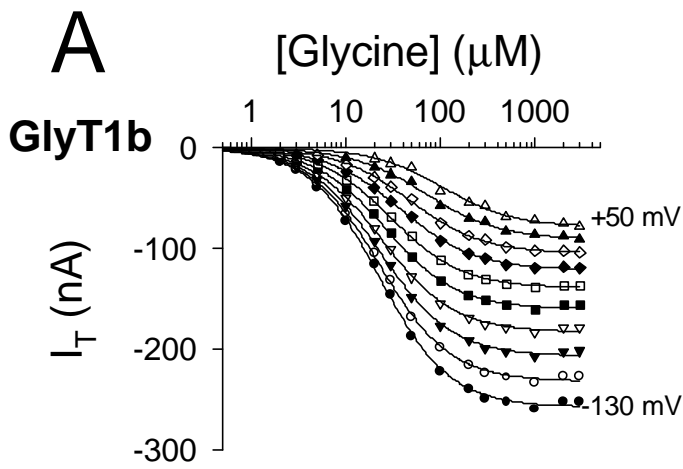
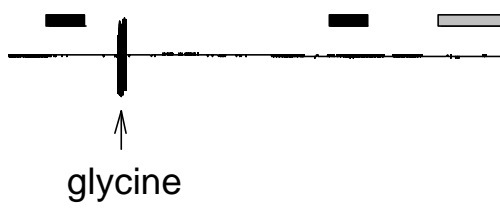


Figure 2

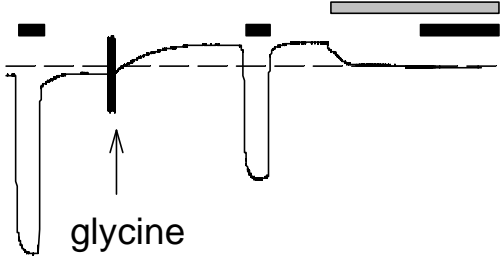


# A Glycine injection

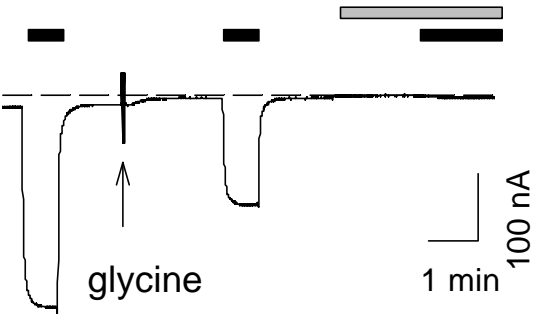
non injected



## GlyT1b

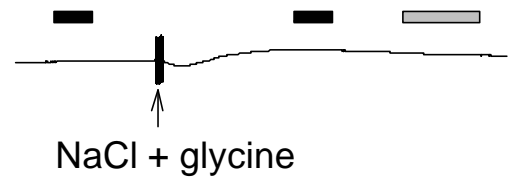


## GlyT2a

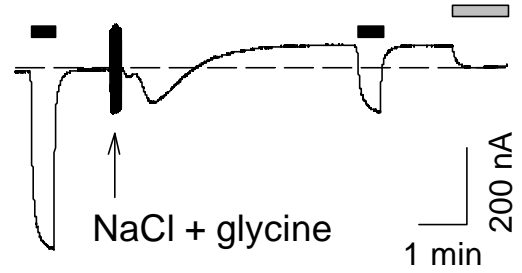


# B Glycine + NaCl injection

non injected



## GlyT2a



# C

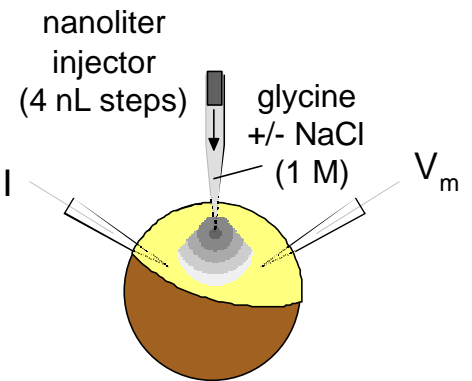


Figure 4

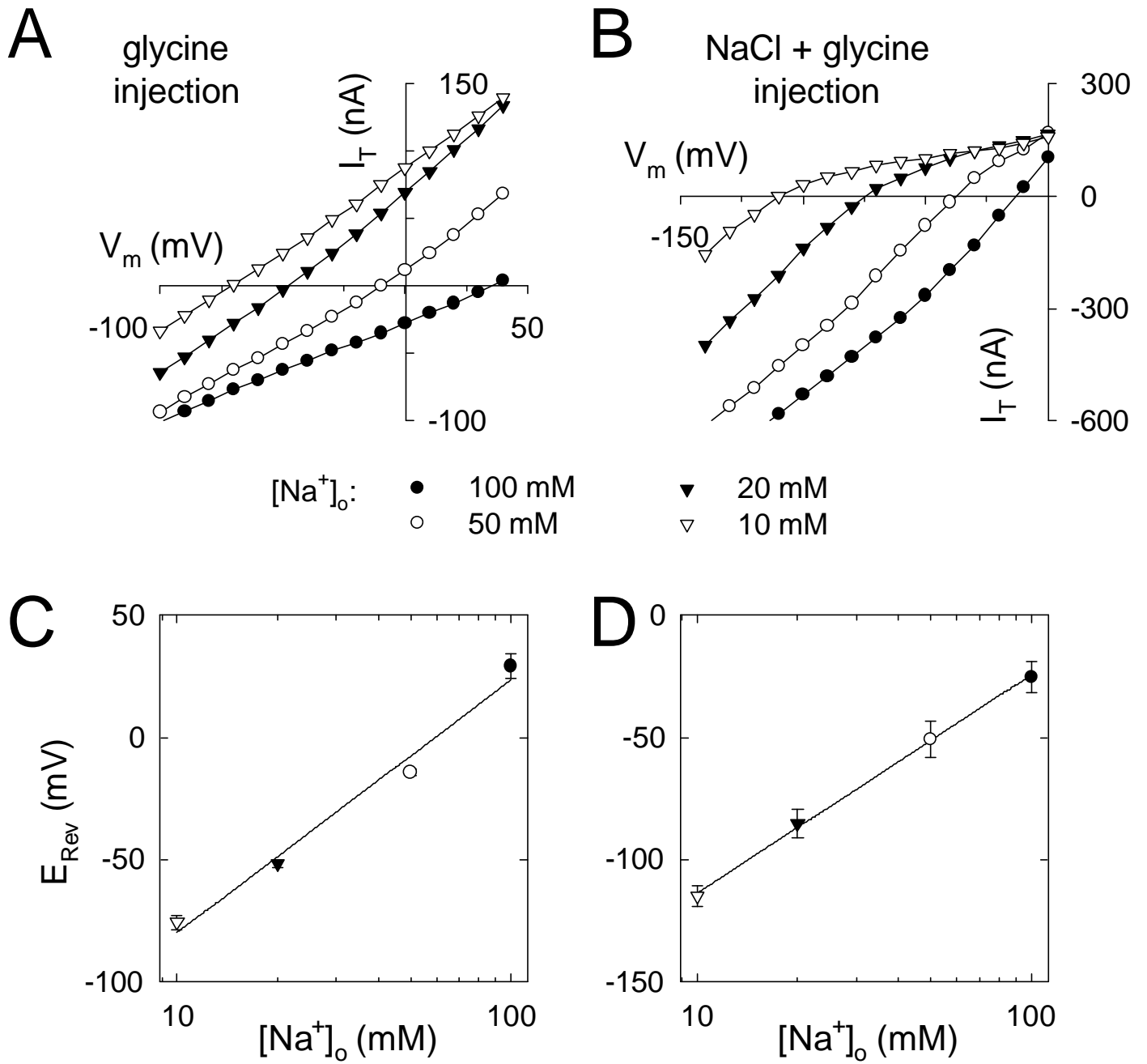


Figure 5

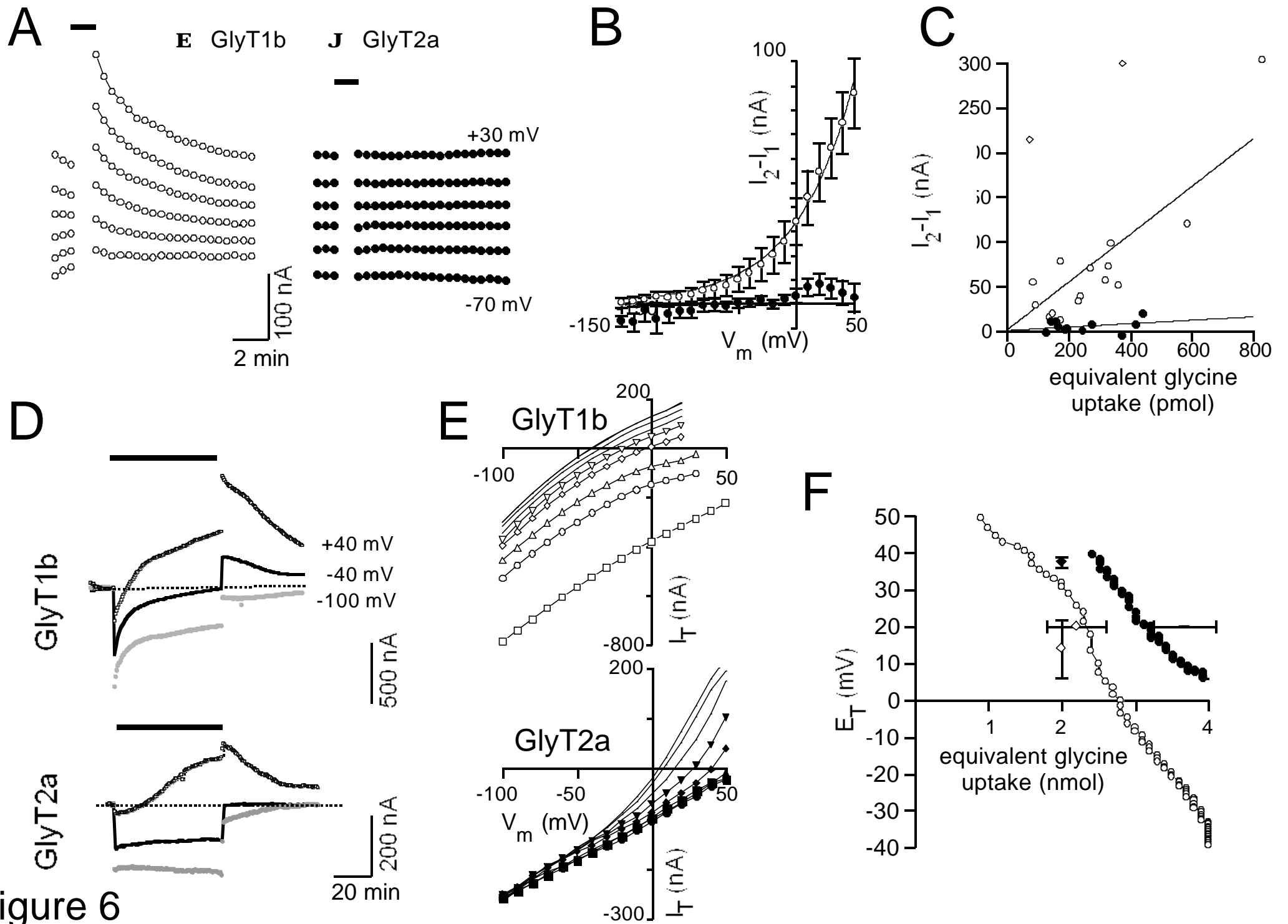
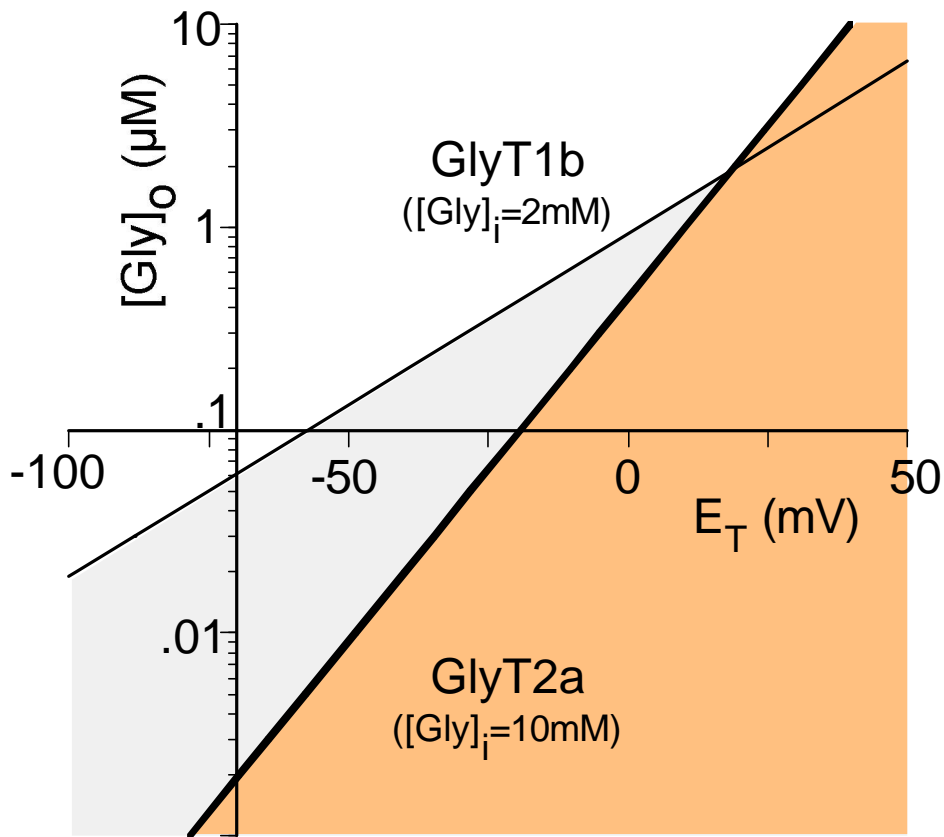


Figure 6

**A**



**B**

